

E-BLOW: E-Beam Lithography Overlapping aware Stencil Planning for MCC System

Bei Yu *Member, IEEE*, Kun Yuan, Jih-Rong Gao, and David Z. Pan *Fellow, IEEE*



Abstract—Electron beam lithography (EBL) is a promising maskless solution for the technology beyond 14nm logic node. To overcome its throughput limitation, industry has proposed character projection (CP) technique, where some complex shapes (characters) can be printed in one shot. Recently the traditional EBL system is extended into multi-column cell (MCC) system to further improve the throughput. In MCC system, several independent CPs are used to further speed-up the writing process. Because of the area constraint of stencil, MCC system needs to be packed/planned carefully to take advantage of the characters. In this paper, we prove that the overlapping aware stencil planning (OSP) problem is NP-hard. To solve OSP problem in MCC system, we present a tool, E-BLOW, with several novel speedup techniques, such as successive relaxation, dynamic programming, and KD-Tree based clustering. Experimental results show that, compared with previous works, E-BLOW demonstrates better performance for both conventional EBL system and MCC system.

Keywords—Electron Beam Lithography, Overlapping aware Stencil Planning, Multi-Column Cell System

1 INTRODUCTION

As the minimum feature size continues to scale to sub-22nm, the conventional 193nm optical photolithography technology is reaching its printability limit. In the near future, multiple patterning lithography (MPL) has become one of the viable lithography techniques for 22nm and 14nm logic nodes [1]–[4]. In the longer future, i.e., for the logic nodes beyond 14nm, extreme ultra violet (EUV), directed self-assembly (DSA), and electric beam lithography (EBL) are promising candidates as next generation lithography technologies [5]. Currently, both EUV and DSA suffer from some technical barriers. EUV technique is delayed due to tremendous technical issues such as lack of power sources, resists, and defect-free masks [6]. DSA has only the potential to generate contact or via layers [7].

The preliminary version has been presented at IEEE/ACM Design Automation Conference (DAC) in 2013.

B. Yu and D. Z. Pan are with the Department of Electrical and Computer Engineering, University of Texas, Austin, TX 78731 USA.

K. Yuan was with the Department of Electrical and Computer Engineering, University of Texas, Austin, TX 78731 USA. He is now with Facebook Inc., Menlo Park, CA 94025 USA.

J-R. Gao was with the Department of Electrical and Computer Engineering, University of Texas, Austin, TX 78731 USA. She is now with Cadence Design Systems, Austin, TX 78752 USA.

EBL system, on the other hand, has been developed for several decades [8]. Compared with the traditional lithographic methodologies, EBL has several advantages. (1) Electron beam can be easily focused into nanometer diameter with charged particle beam, which can avoid suffering from the diffraction limitation of light. (2) The price of a photomask set is getting unaffordable, especially through the emerging MPL techniques. As a maskless technology, EBL can reduce the manufacturing cost. (3) EBL allows a great flexibility for fast turnaround times and even late design modifications to correct or adapt a given chip layout. Because of all these advantages, EBL is being used in mask making, small volume LSI production, and R&D to develop the technological nodes ahead of mass production.

Conventional EBL system applies variable shaped beam (VSB) technique. In this mode, the entire layout is decomposed into a set of rectangles, each being shot into resist by one electron beam. In the printing process of VSB mode, at first the electrical gun generates an initial beam, which becomes uniform through the shaping aperture. Then the second aperture finalizes the target shape with a limited maximum size. Since each pattern needs to be fractured into pieces of rectangles and printed one by one, the VSB mode suffers from serious throughput problem.

One improved technique is called character projection (CP) [9], where the second aperture is replaced by a *stencil*. Some complex shapes, called *characters*, are prepared on the stencil. The key idea is that if a pattern is pre-designed on the stencil, it can be printed in one electronic shot, otherwise it needs to be fractured into a set of rectangles and printed one by one through VSB mode. By this way the CP mode can improve the throughput significantly. In addition, CP exposure has a good CD control stability compared with VSB [10]. However, the area constraint of stencil is the bottleneck. For modern design, due to the numerous distinct circuit patterns, only limited number of patterns can be employed on stencil. Those patterns not contained by stencil are still required to be written by VSB. Thus one emerging challenge in CP mode is how to pack the characters into stencil to effectively improve the throughput.

Even with decades of development, the key limita-

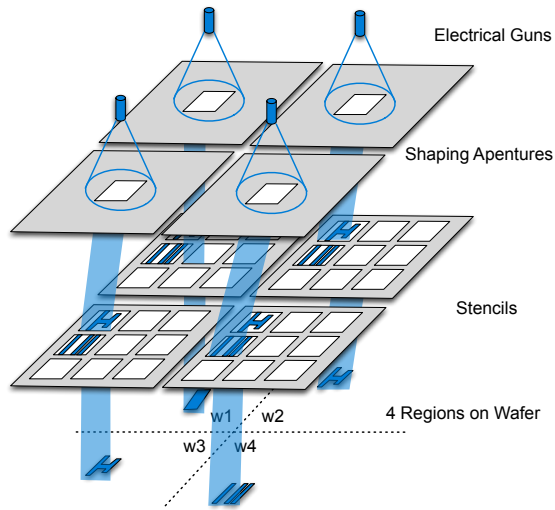


Fig. 1. Printing process of MCC system, where four CPs are bundled.

tion of the EBL system has been and still is the low throughput. Recently, multi-column cell (MCC) system is proposed as an extension to CP technique [11], [12]. In MCC system, several independent character projections (CP) are used to further speed-up the writing process. Each CP is applied on one section of wafer, and all CPs can work parallelly to achieve better throughput. In modern MCC system, there are more than 1300 character projections (CPs) [13]. Since one CP is associated with one stencil, there are more than 1300 stencils in total. The manufacturing of stencil is similar to mask manufacturing. If each stencil is different, then the stencil preparation process would be very time consuming and expensive. Due to the design complexity and cost consideration, different CPs share one stencil design. One example of MCC printing process is illustrated in Fig. 1, where four CPs are bundled to generate an MCC system. In this example, the whole wafer is divided into four regions, w_1, w_2, w_3 and w_4 , and each region is printed through one CP. Note that the whole writing time of the MCC system is determined by the maximum one of the four regions. For modern design, because of the numerous distinct circuit patterns, only limited number of patterns can be employed on stencil. Since the area constraint of stencil is the bottleneck, the stencil should be carefully designed/manufactured to contain the most repeated cells or patterns.

Many previous works dealt with the design optimization for EBL system. [14], [15] considered EBL as a complementary lithography technique to print via/cut patterns. [16], [17] solved the subfield scheduling problem to reduce the critical dimension distortion. [18]–[20] proposed a set of layout/mask fracturing approaches to reduce the VSB shot number. Besides, several works solved the design challenges under CP technique. [21], [22] proposed several character design methods for both

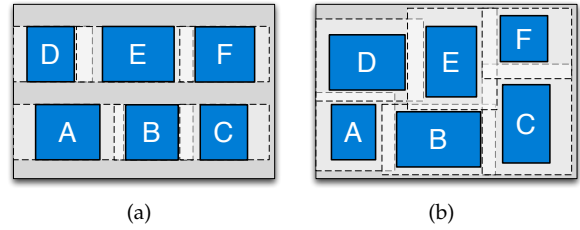


Fig. 2. Two types of OSP problem. (a) 1DOSP. (b) 2DOSP.

via layers and interconnect layers to achieve stencil area-efficiency.

As one of the most challenges in CP mode, stencil planning has earned many attentions [23]–[28]. When blank overlapping is not considered, the stencil planning equals to a character selection problem. [23] proposed an integer linear programming (ILP) formulation to select a group of characters for throughput maximization. When the characters can be overlapped to save more stencil space, the corresponding stencil planning is referred as *overlapping-aware stencil planning* (OSP). [24], [25] investigated on OSP problem to place more characters onto stencil. Recently, [26], [27] assumed that the pattern position in each character can be shifted, and integrated the character re-design into OSP problem. As suggested in [24], the OSP problem can be divided into two types: 1DOSP and 2DOSP. In 1DOSP, the standard cells with same height are selected into stencil. As shown in Fig. 2(a), each character implements one standard cell, and the enclosed circuit patterns of all the characters have the same height. Note that here we only show the horizontal blanks, and the vertical blanks are not represented because they are identical. In 2DOSP, the blank spaces of characters are non-uniform along both horizontal and vertical directions. By this way, stencil can contain both complex via patterns and regular wires. Fig. 2(b) illustrates a stencil design example for 2DOSP.

Compared with conventional EBL system, MCC system introduces two main challenges in OSP problem. First, the objective is new: in MCC system the wafer is divided into several regions, and each region is written by one CP. Therefore the new OSP should minimize the maximal writing times of all regions. However, in conventional EBL system the objective is simply minimize the wafer writing time. Besides, the stencil for an MCC system can contain more than 4000 characters, previous methodologies for EBL system may suffer from runtime penalty. However, no existing stencil planning work has been done toward the MCC system.

This paper presents E-BLOW, a comprehensive study to the MCC system 1DOSP and 2DOSP problems. Our main contributions are summarized as follows.

- We provide the proof that both 1DOSP and 2DOSP problems are NP-hard.
- We formulate integer linear programming (ILP) to co-optimizing characters selection and physi-

cal placements on stencil. To our best knowledge, this is the first mathematical formulation for both 1DOSP and 2DOSP.

- We propose a simplified formulation for 1DOSP.
- We present a successive relaxation algorithm to find a near optimal solution.
- We design a KD-Tree based clustering algorithm to speedup 2DOSP solution.

The rest of this paper is organized as follows. Section 2 provides problem formulation. Section 3 presents algorithmic details to resolve 1DOSP problem in E-BLOW, while section 4 details the E-BLOW solutions to 2DOSP problem. Section 5 reports experimental results, followed by the conclusion in Section 6.

2 PRELIMINARIES

In this section, we provide the preliminaries regarding overlapping aware stencil planning (OSP). During character design, blank area is usually reserved around its boundaries. Note in this paper, the blank space refers to the blank around the character boundaries. The term “overlapping” means sharing blanks between adjacent characters. By this way, more characters can be placed on the stencil [24]. In this section, first we will provide the detailed problem formulation, then we will prove that both 1DOSP and 2DOSP are NP-hard.

2.1 Problem Formulation

In an MCC system with P CPs, the whole wafer is divided into P regions $\{r_1, r_2, \dots, r_P\}$, and each region is written by one particular CP. We assume cell extraction [29] has been resolved first. In other words, a set of character candidates $\{c_1, \dots, c_n\}$ has already been given to the MCC system. For each character candidate c_i , its writing time through VSB mode is denoted as n_i , while its writing time through CP mode is 1.

The regions of wafer have different layout patterns, and the throughputs would be also different. Suppose character candidate c_i repeats t_{ic} times on region r_c . Let a_i indicate the selection of character candidate c_i as follows.

$$a_i = \begin{cases} 1, & \text{candidate } c_i \text{ is selected on stencil} \\ 0, & \text{otherwise} \end{cases}$$

If c_i is prepared on stencil, the total writing time of pattern c_i on region r_c is $t_{ic} \cdot 1$. Otherwise, c_i should be printed through VSB. Since region r_c comprises t_{ic} candidate c_i , the writing time would be $t_{ic} \cdot n_i$. Therefore, for region r_c the total writing time T_c is as follows:

$$\begin{aligned} T_c &= \sum_{i=1}^n a_i \cdot (t_{ic} \cdot 1) + \sum_{i=1}^n (1 - a_i) \cdot (t_{ic} \cdot n_i) \\ &= \sum_{i=1}^n t_{ic} \cdot n_i - \sum_{i=1}^n t_{ic} \cdot (n_i - 1) \cdot a_i \\ &= T_c^{VSB} - \sum_{i=1}^n R_{ic} \cdot a_i \end{aligned}$$

where we denote $T_c^{VSB} = \sum_{i=1}^n t_{ic} \cdot n_i$, and $R_{ic} = t_{ic} \cdot (n_i - 1)$. T_c^{VSB} shows the writing time on r_c when only VSB is applied, and R_{ic} represents the writing time reduction of candidate c_i on region r_c . In MCC system, for each region r_c both T_c^{VSB} and R_{ic} are constants. Therefore, the total writing time of the MCC system is formulated as follows:

$$\begin{aligned} T_{total} &= \max\{T_c\} \\ &= \max\{T_c^{VSB} - \sum_{i=1}^n R_{ic} \cdot a_i\}, \forall c \in P \end{aligned} \quad (1)$$

Based on the notations above, we define the overlapping aware stencil planning (OSP) for MCC system as follows.

Problem 1. OSP for MCC System: Given a set of character candidate C^C , select a subset C^{CP} out of C^C as characters, and place them on the stencil. The objective is to minimize the system writing time T_{total} expressed by Eqn. (1), while the placement of C^{CP} is bounded by the outline of stencil. The width and height of stencil is W and H , respectively.

For convenience, we use the term OSP to refer OSP for MCC system in the rest of this paper.

2.2 NP-Hardness

In this subsection we will prove that both 1DOSP and 2DOSP are NP-hard. To facilitate the proof, we first define a Bounded Subset Sum (BSS) problem as follows.

Problem 2 (Bounded Subset Sum). Given a list of n numbers x_1, \dots, x_n and a number s , where $\forall i \in [n] \ 2 \cdot x_i > x_{\max} (\triangleq \max_{i \in [n]} |x_i|)$, decide if there is a subset of the numbers that sums up to s .

For example, given three numbers 1100, 1200, 1413 and $T = 2300$, we can find a subset $\{1100, 1200\}$ such that $1100 + 1200 = 2300$. Additionally, we can assumption that $t > c \cdot x_{\max}$, where c is some constant. Otherwise it be solved in $O(n^c)$ time. Besides, without the bounded constraint $\forall i \in [n] \ 2 \cdot x_i > x_{\max}$, the BSS problem becomes **Subset sum** problem, which is in NP-complete [30]. For simplicity of later explanation, let S denote the set of n numbers. Note that, we can assume that all the numbers are integer numbers.

Theorem 1. BSS problem is NP-complete.

The proof is in Appendix. In the following, we will show that even a simpler version of 1DOSP problem is NP-hard. In this simpler version, there is only one row in the stencil, and a set of characters C is given. Besides, the blanks of each character are symmetric, and each character $c_i \in C$ is with the same length w .

Definition 1 (Minimum packing). Given a subset of characters $C' \in C$, its minimum packing is the packing with the minimum stencil length.

Lemma 1. Given a set of character $C = \{c_1, c_2, \dots, c_n\}$ placed on a single row stencil. If for each character $c_i \in C$, both of its left and right blanks are s_i , then the minimum packing is with the following stencil length

$$n \cdot M - \sum_{i=1}^n s_i + \max_{i \in [n]} \{s_i\} \quad (2)$$

Proof. Without loss of generality, we assume that $s_1 \geq s_2 \geq \dots \geq s_n$. We prove by recursion that in a minimum length packing, the overlapping blank is $f(n) = \sum_{i=2}^n s_i$. If there are only two characters, it is trivial that $f(2) = s_2$. We assume that when $p = n - 1$, the maximum overlapping blank $f(n - 1) = \sum_{i=2}^{n-1} s_i$. For the last character c_n , the maximum sharing blank value is s_n . Since for any $i < n$, $s_i \geq s_n$, we can simply insert it at either the left end or the right end, and find the incremental overlapping blank s_n . Thus $f(n) = f(n - 1) + s_n = \sum_{i=2}^n s_i$. Because the maximum overlapping blank for all characters is $\sum_{i=2}^n s_i$, we can see the minimum packing length is as in Eqn. (2). \square

Lemma 2. BSS \leq_p 1DOSP.

Proof. Given an instance of BSS with s and $S = \{x_1, x_2, \dots, x_n\}$, we construct a 1DOSP instance as follows:

- The stencil length is set to $M + s$, where $M = \max_{i \in [n]} \{x_i\}$.
- For each $x_i \in S'$, in 1DOSP there is a character c_i , whose width is M and both left and right blanks are $M - x_i$. Since $x_i > M/2$, the sum of left blank and right blank is less or equal to M .
- We introduce an additional character c_0 , whose width size is M , and both left and right blanks are $M - \min_{i \in [n]} \{x_i\}$.
- The VSB writing time of character c_0 is set to $\sum_{i \in [n]} x_i$, while the VSB writing time for each character c_i is set to x_i . The CP writing times are set to 0 for all characters.
- There is only one region, and each character c_i repeats one time in the region.

For instance, given initial set $S = \{1100, 1200, 2000\}$ and $s = 2300$, the constructed 1DOSP instance is shown in Fig. 3.

We will show the BSS instance $S = \{x_1, x_2, \dots, x_n\}$ has a subset that adds up to s if and only if the constructed 1DOSP instance has minimum packing length $M + s$ and total writing time smaller than $\sum x_i$.

(\Rightarrow part) After solving the BSS problem, a set of items S' are selected that they add up to s . For each $x_i \in S'$, character c_i is also selected into the stencil. Besides, since the system writing time for c_0 is $\sum x_i$, it is trivial to see that in the 1DOSP instance the c_0 must be selected. Due to the Lemma 1, the minimum total packing length is

$$(n + 1) \cdot M - \sum_{i \in S'} (M - x_i) = M + \sum_{i \in S'} x_i = M + s$$

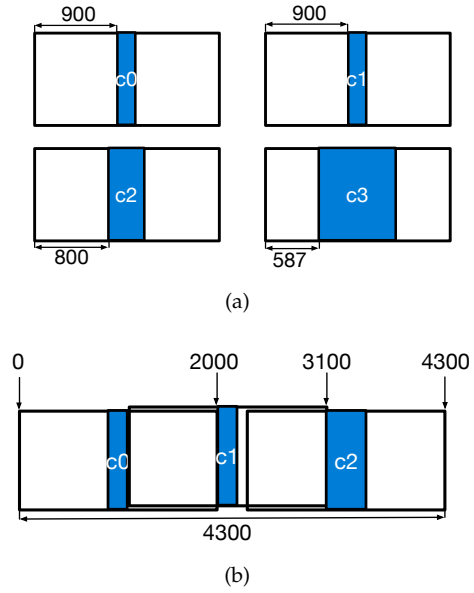


Fig. 3. (a) 1DOSP instance for the BSS instance $S = \{1100, 1200, 2000\}$ and $s = 2300$. (b) The minimum packing is with stencil length $M + s = 2000 + 2300 = 4300$.

Meanwhile, the minimum total writing time in the 1DOSP is $\sum x_i - s$.

(\Leftarrow part) We start from a 1DOSP instance with minimum packing length $M + s$ and total writing time smaller than $\sum x_i$, where a set of character $C' \in C$ are selected. Since the total writing time must be smaller than $\sum x_i$, character $c_0 \in C'$. For all characters in set $c_i \in C'$ except c_0 , we select x_i into the subset $S' \in S$, which adds up to s . \square

Theorem 2. 1DOSP is in NP-hard.

Proof. Directly from Lemma 2 and Theorem 1. \square

Theorem 3. 2DOSP is in NP-hard.

Since 1DOSP is a special case of 2DOSP. Due to the NP-hardness of 1DOSP, the 2DOSP problem is NP-hard as well. Combining Theorem 2 and Theorem 3, we can achieve the conclusion that OSP problem, even for conventional EBL system, is NP-hard.

3 E-BLOW FOR 1DOSP

When each character implements one standard cell, the enclosed circuit patterns of all the characters have the same height. The corresponding OSP problem is called 1DOSP, which can be viewed as a combination of character selection and single row ordering problems [24]. Different from two-step heuristic proposed in [24], we show that these two problems can be solved simultaneously through a unified ILP formulation (3). For convenience, Table 1 lists the notations used in 1DOSP problem.

TABLE 1
Notations used in 1D-ILP Formulation

W	width constraint of stencil or row
n	number of characters
m	number of rows
x_i	x-position of character c_i
w_i	width of character c_i
o_{ij}^h	horizontal overlap between c_i and c_j
p_{ij}	0-1 variable, $p_{ij} = 0$ if c_i is left of c_j
a_{ij}	0-1 variable, $a_{ij} = 1$ if c_i is on j th row

$$\min T_{total} \quad (3)$$

$$\text{s.t. } T_{total} \geq T_c^{VSB} - \sum_{i=1}^n \left(\sum_{k=1}^m R_{ic} \cdot a_{ik} \right) \quad \forall c \in P \quad (3a)$$

$$0 \leq x_i \leq W - w_i \quad \forall i \quad (3b)$$

$$\sum_{k=1}^m a_{ik} \leq 1 \quad \forall i \quad (3c)$$

$$x_i + w_{ij} - x_j \leq W(2 + p_{ij} - a_{ik} - a_{jk}) \quad \forall i, j \quad (3d)$$

$$x_j + w_{ji} - x_i \leq W(3 - p_{ij} - a_{ik} - a_{jk}) \quad \forall i, j \quad (3e)$$

$$a_{ik}, a_{jk}, p_{ij} : 0 - 1 \text{ variable} \quad \forall i, j \quad (3f)$$

In formulation (3), W is the stencil width, m is the number of rows. For each character c_i , w_i and x_i are the width and the x-position, respectively. If and only if c_i is assigned to k -th row, $a_{ik} = 1$. Otherwise, $a_{ik} = 0$. Constraints (3d) (3e) are used to check position relationship between c_i and c_j . Here $w_{ij} = w_i - o_{ij}^h$ and $w_{ji} = w_j - o_{ji}^h$, where o_{ij}^h is the overlapping when candidates c_i and c_j are packed together. Only when $a_{ik} = a_{jk} = 1$, i.e. both character i and character j are assigned to row k , one of the two constraints (3d) (3e) will be active. Besides, for any three characters c_1, c_2, c_3 being assigned to row k , i.e., $a_{1k} = a_{2k} = a_{3k} = 1$, the p_{12}, p_{13} and p_{23} are self-consistent. That is, if c_1 is on the left of c_2 ($p_{12} = 0$) and c_2 is on the left of c_3 ($p_{23} = 0$), then c_1 should be on the left of c_3 ($p_{13} = 0$). Similarly, if c_1 is on the right of c_2 ($p_{12} = 1$) and c_2 is on the right of c_3 ($p_{23} = 1$), then c_1 should be on the right of c_3 ($p_{13} = 1$) as well.

Since ILP is a well known NP-hard problem, directly solving it may suffer from long runtime penalty. One straightforward speedup method is to relax the ILP into the corresponding linear programming (LP) through replacing constraints (3f) by the following:

$$0 \leq a_{ik}, a_{jk}, p_{ij} \leq 1$$

It is obvious that the LP solution provides a lower bound to the ILP solution. However, we observe that the solution of relaxed LP could be like this: for each i , $\sum_j a_{ij} = 1$ and all the p_{ij} are assigned 0.5. Although the objective function is minimized and all the constraints are satisfied, this LP relaxation provides no useful information to guide future rounding, i.e., all the character

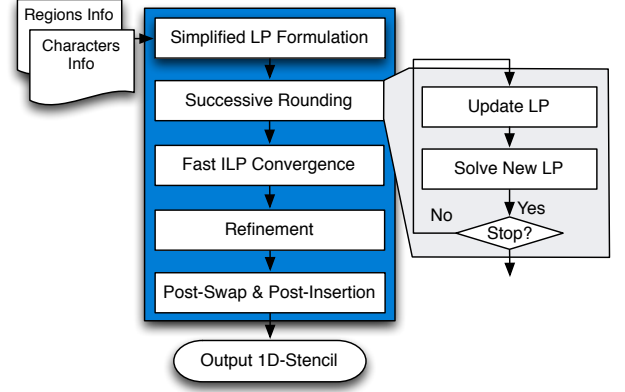


Fig. 4. E-BLOW overall flow for 1DOSP.

candidates are selected and no ordering relationship is determined.

To overcome the limitation of above rounding, E-BLOW proposes a novel successive rounding framework to search near-optimal solution in reasonable runtime. As shown in Fig. 4, the overall flow includes several steps: Simplified ILP formulation, Successive Rounding, Fast ILP Convergence, Refinement, Post-swap and Post-Insertion. In section 3.1 the simplified formulation will be discussed, and its LP rounding lower bound will be proved. In section 3.2 the details of successive rounding would be introduced. In section 3.3 the Fast ILP convergence technique would be presented. In section 3.4 the refinement process is proposed. At last, to further improve the performance, in section 3.5 the post-swap and post-insertion techniques are discussed.

3.1 Simplified ILP Formulation

As discussed above, solving the ILP formulation (3) is very time consuming, and the related LP relaxation may be bad in performance. To overcome the limitations of (3), in this section we introduce a simplified ILP formulation, whose LP relaxation can provide good lower bound. The simplified formulation is based on a *symmetrical blank* (S-Blank) assumption: the blanks of each character are symmetric, i.e., left blank equals to right blank. s_i is used to denote the blank of character c_i . Note that for different characters c_i and c_j , their blanks s_i and s_j can be different.

At first glance the S-Blank assumption may lose optimality. However, it provides several practical and theoretical benefits. (1) In [24] the single row ordering problem was transferred into Hamilton Cycle problem, which is a well known NP-hard problem and even particular solver is quite expensive. In our work, instead of relying on expensive solver, under this assumption the problem can be optimally solved in $O(n)$. (2) Under S-Blank assumption, the ILP formulation can be effectively simplified to provide a reasonable rounding bound

$$\max \sum_i \sum_j a_{ij} \cdot profit_i \quad (4)$$

$$\text{s.t. } \sum_i (w_i - s_i) \cdot a_{ij} \leq W - B_j \quad \forall j \quad (4a)$$

$$B_j \geq s_i \cdot a_{ij} \quad \forall i, j \quad (4b)$$

$$\sum_j a_{ij} \leq 1 \quad \forall i \quad (4c)$$

$$a_{ij} = 0 \text{ or } 1 \quad \forall i, j \quad (4d)$$

theoretically. Compared with previous heuristic framework [24], the proved rounding bound provides a better guideline for a global view search. (3) To compensate the inaccuracy in the asymmetrical blank cases, E-BLOW provides a refinement (see section 3.4).

The simplified ILP formulation is shown in Eqn. (4).

In the objective function of Eqn. (4), each character c_i is associated with one profit value $profit_i$. The $profit_i$ value is to evaluate the overall system writing time improvement if character c_i is selected. Through assigning each character c_i with one profit value, we can simplify the complex constraint (3a). More details regarding the profit value setting would be discussed in Section 3.2. Besides, due to Lemma 1, constraint (4a) and constraint (4b) are for row width calculation, where (4b) is to linearize max operation. Here B_j can be viewed as the maximum blank space of all the characters on row r_j . Constraint (4c) implies each character can be assigned into at most one row. It's easy to see that the number of variables is $O(nm)$, where n is the number of characters, and m is the number of rows. Generally speaking, single character number n is much larger than row number m . Thus compared with basic ILP formulation (3), the variable number in (4) can be reduced dramatically.

In our implementation, we set s_i to $\lceil (sl_i + sr_i)/2 \rceil$, where sl_i and sr_i are c_i 's left blank and right blank, respectively. Note that here the ceiling function is used to make sure that under the S-Blank assumption, each blank is still integral. Although this setting may loss some optimality, E-BLOW provides post-stage to compensate the inaccuracy through incremental character insertion.

Now we will show that the LP relaxation of (4) has reasonable lower bound. To explain this, let us first look at a similar formulation (5) as follows:

$$\max \sum_i \sum_j a_{ij} \cdot profit_i \quad (5)$$

$$\text{s.t. } \sum_i (w_i - s_i) \cdot a_{ij} \leq W - max_s \quad \forall j \quad (5a)$$

$$(4c) - (4d)$$

where max_s is the maximum horizontal blank length of every character, i.e. $max_s = \max\{s_i | i = 1, 2, \dots, n\}$. Program (5) is a multiple knapsack problem [31]. A multiple knapsack is similar to a knapsack problem, with the difference that there are multiple knapsacks.

Algorithm 1 SuccRounding (th_{inv})

Require: ILP Formulation (4)

```

1: Set all  $a_{ij}$  as unsolved;
2: repeat
3:   Update  $profit_i$  for all unsolved  $a_{ij}$ ;
4:   Solve relaxed LP of (4);
5:   repeat
6:      $a_{pq} \leftarrow \max\{a_{ij}\}$ ;
7:     for all  $a_{ij} \geq a_{pq} \times th_{inv}$  do
8:       if  $c_i$  can be assigned to row  $r_j$  then
9:          $a_{ij} = 1$  and set it as solved;
10:        Update capacity of row  $r_j$ ;
11:       end if
12:     end for
13:   until cannot find  $a_{pq}$ 
14: until

```

In formulation (5), each $profit_i$ can be rephrased as $(w_i - s_i) \times ratio_i$.

Lemma 3. *If each $ratio_i$ is the same, the multiple knapsack problem (5) can find a 0.5-approximation algorithm using LP rounding method.*

For brevity we omit the proof, detailed explanations can be found in [32]. When all $ratio_i$ are the same, formulation (5) can be approximated to a max-flow problem. In addition, if we denote α as $\min\{ratio_i\} / \max\{ratio_i\}$, we can achieve the following Lemma:

Lemma 4. *The LP rounding solution of (5) can be a 0.5α -approximation to optimal solution of (5).*

Proof: First we introduce a modified formulation to program (5), where each $profit_i$ is set to $\min\{profit_i\}$. In other words, in the modified formulation, each $ratio_i$ is the same. Let OPT and OPT' be the optimal values of (5) and the modified formulation, respectively. Let APR' be the corresponding LP rounding result in the modified formulation. According to Lemma 3, $APR' \geq 0.5 \cdot OPT'$. Since $\min\{profit_i\} \geq profit_i \cdot \alpha$, we can get $OPT' \geq \alpha \cdot OPT$. In summary, $APR' \geq 0.5 \cdot OPT' \geq 0.5\alpha \cdot OPT$. \square

The difference between (4) and (5) is the right side values at (4a) and (5a). Blank spacing is relatively small comparing with the row length, we can get that $W - max_s \approx W - B_j$. Then we can expect that program (4) has a reasonable rounding performance.

3.2 Successive Rounding

In this subsection we propose a successive rounding algorithm to solve program (4) iteratively. Successive rounding uses a simple iterative scheme in which fractional variables are rounded one after the other until an integral solution is found [33]. The ILP formulation (4) becomes an LP if we relax the discrete constraint to a continuous constraint as: $0 \leq a_{ij} \leq 1$.

The details of successive rounding is shown in Algorithm 1. At first we set all a_{ij} as *unsolved* since none of them is assigned to rows. The LP is updated and solved iteratively. For each new LP solution, we search the maximal a_{ij} , and store in a_{pq} (line 6). Then we find all a_{ij} that is closest to the maximum value a_{pq} , i.e., $a_{ij} \geq a_{pq} \times th_{innv}$. In our implementation, th_{innv} is set to 0.9. For each selected variables a_{ij} , we try to pack c_i into row r_j , and set a_{ij} as *solved*. Note that when one character c_i is assigned to one row, all a_{ij} would be set as solved. Therefore, the variable number in updated LP formulation would continue to decrease. This procedure repeats until no appropriate a_{ij} can be found. One key step of Algorithm 1 is the $profit_i$ update (line 3). For each character c_i , we set its $profit_i$ as follows:

$$profit_i = \sum_c \frac{t_c}{t_{max}} \cdot (n_i - 1) \cdot t_{ic} \quad (6)$$

where t_c is current writing time of region r_c , and $t_{max} = \max \{t_c, \forall c \in P\}$. Through applying the $profit_i$, the region r_c with longer writing time would be considered more during the LP formulation. During successive rounding, if c_i is not assigned to any row, $profit_i$ would continue to be updated, so that the total writing time of the whole MCC system can be minimized.

3.3 Fast ILP Convergence

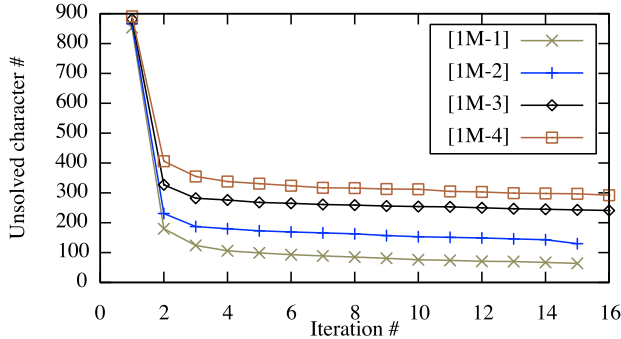


Fig. 5. Unsolved character number along the LP iterations for testcases 1M-1, 1M-2, 1M-3, and 1M-4.

During successive rounding, for each LP iteration, we select some characters into rows, and set these characters as solved. In the next LP iteration, only unsolved characters would be considered in formulation. Thus the number of unsolved characters continues to decrease through the iterations. For four test cases (1M-1 to 1M-4), Fig. 5 illustrates the number of unsolved characters in each iteration. We observe that in early iterations, more characters would be assigned to rows. However, when the stencil is almost full, fewer of a_{ij} could be close to 1. Thus, in late iterations only few characters would be assigned into stencil, and the successive rounding requires more iterations.

To overcome this limitation so that the successive rounding iteration number can be reduced, we present

Algorithm 2 Fast ILP Convergence (L_{th}, U_{th})

Require: Solutions of relaxed LP (4);

- 1: **for all** a_{ij} in relaxed LP solutions **do**
- 2: **if** $a_{ij} < L_{th}$ **then**
- 3: Set a_{ij} as solved;
- 4: **end if**
- 5: **if** $a_{ij} > U_{th}$ **then**
- 6: Assign c_i to row r_j ;
- 7: Set a_{ij} as solved;
- 8: **end if**
- 9: **end for**
- 10: Solve ILP formulation (4) for all unsolved a_{ij}
- 11: **if** $a_{ij} = 1$ **then**
- 12: Assign c_i to row r_j ;
- 13: **end if**

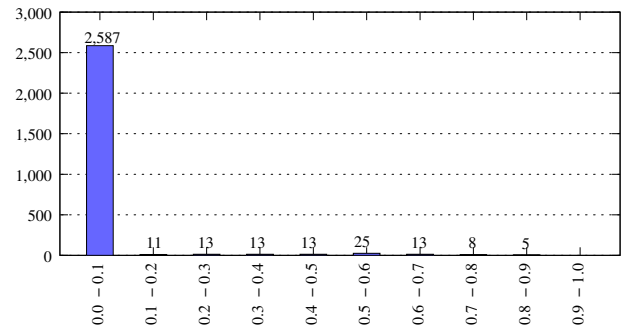


Fig. 6. For test case 1M-1, solution distribution in last LP, where most of values are close to 0.

a convergence technique based on fast ILP formulation. The basic idea is that when we observe only few characters are assigned into rows in one LP iteration, we stop successive rounding in advance, and call fast ILP convergence to assign all left characters. Note that in [25] an ILP formulation with similar idea was also applied. The details of the ILP convergence is shown in Algorithm 2. The input are the solutions of last LP rounding, and two parameters L_{th} and U_{th} . First we check each a_{ij} (lines 1-9). If $a_{ij} < L_{th}$, then we assume character c_i would be not assigned to row r_j , and set a_{ij} as solved. Similarly, if $a_{ij} > U_{th}$, we assign c_i to row r_j and set a_{ij} as solved. For those unsolved a_{ij} we build up ILP formulation (4) to assign final rows (lines 10-13).

At first glance the ILP formulation may be expensive to solve. However, we observe that in our convergence Algorithm 2, typically the variable number is small. Fig. 6 illustrates the solution distribution in last LP formulation. We can see that most of the values are close to 0. In our implementation L_{th} and U_{th} are set to 0.1 and 0.9, respectively. For this case, although the LP formulation contains more than 2500 variables, our fast ILP formulation results in only 101 binary variables.

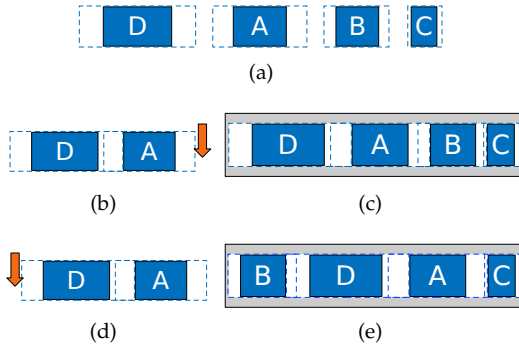


Fig. 7. Greedy based Single Row Ordering. (a) At first all candidates are sorted by blank space. (c) One possible ordering solution where each candidate chooses the right end position. (e) Another possible ordering solution.

3.4 Refinement

Refinement is a stage to solve the single row ordering problem [24], which adjusts the relative locations of input p characters to minimize the total width. Under the S-Blank assumption, because of Lemma 1, this problem can be optimally solved through the following two-step greedy approach.

- 1) All characters are sorted decreasingly by blanks;
- 2) All characters are inserted one by one. Each one can be inserted at either left end or right end.

One example of the greedy approach is illustrated in Fig. 7, where four character candidates A, B, C and D are to be ordered. In Fig. 7(a), they are sorted decreasingly by blank space. Then all the candidates are inserted one by one. From the second candidate, each insertion has two options: left side or right side of the whole packed candidates. For example, if A is inserted at the right of D , B has two insertion options: one is at the right side of A (Fig. 7(b)), another is at the left side of A (Fig. 7(d)). Given different choices of candidate B , Fig. 7(c) and Fig. 7(e) give corresponding final solutions. Since from the second candidate each one has two choices, by this greedy approach n candidates will generate 2^{n-1} possible solutions.

For the asymmetrical cases, the optimality does not hold anymore. To compensate the losing, E-BLOW consists of a refinement stage. For n characters $\{c_1, \dots, c_n\}$, single row ordering can have $n!$ possible solutions. We avoid enumerating such huge solutions, and take advantage of the order in symmetrical blank assumption. That is, we pick up one best solution from the 2^{n-1} possible ones. Noted that although considering 2^{n-1} instead of $n!$ options cannot guarantee optimal single row packing, our preliminary results show that the solution quality loss is negligible in practice.

The refinement is based on dynamic programming, and the details are shown in Algorithm 3. Refine(k) generates all possible order solutions for the first k characters $\{c_1, \dots, c_k\}$. Each order solution is represented

as a set (w, l, r, O) , where w is the total length of the order, l is the left blank of the left character, r is the right blank of the right character, and O is the character order. At the beginning, an empty solution set S is initialized (line 1). If $k = 1$, then an initial solution $(w_1, sl_1, sr_1, \{c_1\})$ would be generated (line 2). Here w_1, sl_1 , and sr_1 are width of first character c_1 , left blank of c_1 , and right blank of c_1 . If $k > 1$, then *Refine*(k) will recursively call *Refine*($k-1$) to generate all old partial solutions. All these partial solutions will be updated by adding candidate c_k (lines 5-9).

Algorithm 3 Refine(k)

Require: k characters $\{c_1, \dots, c_k\}$;

- 1: **if** $k = 1$ **then**
 - 2: Add $(w_1, sl_1, sr_1, \{c_1\})$ into S ;
 - 3: **else**
 - 4: Refine($k-1$);
 - 5: **for** each partial solution (w, l, r, O) **do**
 - 6: Remove (w, l, r, O) from S ;
 - 7: Add $(w + w_k - \min(sr_k, l), sl_k, r, \{c_k, O\})$ into S ;
 - 8: Add $(w + w_k - \min(sl_k, r), l, sr_k, \{O, c_k\})$ into S ;
 - 9: **end for**
 - 10: **if** size of $S \geq threshold$ **then**
 - 11: Prune inferior solutions in S ;
 - 12: **end if**
 - 13: **end if**
-

We propose pruning techniques to speed-up the dynamic programming process. Let us introduce the concept of inferior solutions. For any two solutions $S_A = (w_a, l_a, r_a, O_a)$ and $S_B = (w_b, l_b, r_b, O_b)$, we say S_B is **inferior** to S_A if and only if $w_a \geq w_b$, $l_a \leq l_b$ and $r_a \leq r_b$. Those inferior solutions would be pruned during pruning section (lines 10-12). In our implementation, the *threshold* is set to 20.

3.5 Post-Swap and Post-Insertion

After refinement, a post-swap stage is applied to further improve the performance. In each swap operation, an unselected character would be swapped with a character on stencil, if such swap can improve the writing time. The post-swap is implemented using a greedy flavor that consists of two steps. First, all the unselected characters are sorted. Second, the unselected characters would try to swap with the characters on stencils one by one.

After post-swap, a post-insertion stage is applied to further insert more characters into stencil. Different from the greedy insertion approach in [24] that new characters can be only inserted into one row's right end. We consider to insert characters into the middle part of rows. Generally speaking, the character with higher profit value (6) would have a higher priority to be inserted into rows. We propose a character insertion algorithm to insert some additional characters into the rows.

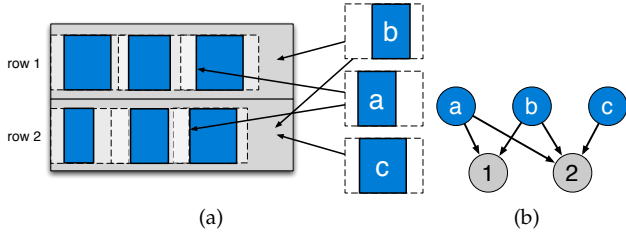


Fig. 8. Example of maximum weighted matching based post character insertion. (a) Three additional characters a, b, c and two rows. (b) Corresponding bipartite graph to represent the relationships among characters and rows.

The insertion is formulated as a maximum weighted matching problem [34], under the constraint that for each row there is at most one character can be inserted. Although this assumption may loss some optimality, in practical it works quite well as usually the remaining space for a row is very limited.

Fig. 8 illustrates one example of the character insertion. As shown in Fig. 8 (a), there are two rows (row 1, row 2) and three additional characters (a, b, c). Characters a and b can be inserted into either row 1 or row 2, but character c can only be inserted into row 2. It shall be noted that the insertion position is labeled by arrows. For example, two arrows from character a mean that a can be inserted into the middle of each row. We build up a bipartite graph to represent the relationships among characters and rows (see Fig. 8 (b)). Each edge is associated with a cost as character's profit. By utilizing the bipartite graph, the best character insertion can be solved by finding a maximum weighted matching.

Given n additional characters, we search the possible insertion positions under each row. The time complexity of searching all the possibilities is $O(nmC)$, where m is the total row number and C is the maximum character number on each row. We propose two heuristics to speed-up the search process. First, to reduce n , we only consider those additional characters with high profits. Second, to reduce m , we skip those rows with very little empty space.

4 E-BLOW FOR 2DOSP

Now we consider a more general case: the blank spaces of characters are non-uniform along both horizontal and vertical directions. This problem is referred to 2DOSP problem. In [24] the 2DOSP problem was transformed into a floorplanning problem. However, several key differences between traditional floorplanning and OSP were ignored. (1) In OSP there is no wirelength to be considered, while at floorplanning wirelength is a major optimization objective. (2) Compared with complex IP cores, lots of characters may have similar sizes. (3) Traditional floorplanner could not handle the problem size of modern MCC design.

TABLE 2
Notations used in 2D-ILP Formulation

$W(H)$	width (height) constraint of stencil
$w_i(h_i)$	width (height) of candidate c_i
$o_{ij}^h(o_{ij}^v)$	horizontal (vertical) overlap between c_i and c_j
$w_{ij}(h_{ij})$	$w_{ij} = w_i - o_{ij}^h, h_{ij} = h_i - o_{ij}^v$
a_i	0-1 variable, $a_i = 1$ if c_i is on stencil

4.1 ILP Formulation

Here we will show that 2DOSP can be formulated as integer linear programming (ILP) as well. Compared with 1DOSP, 2DOSP is more general: the blank spaces of characters are non-uniform along both horizontal and vertical directions. The 2DOSP problem can be also formulated as an ILP formulation (7). For convenience, Table 2 lists some notations used in the ILP formulation. The formulation is motivated by [35], but the difference is that our formulation can optimize both placement constraints and character selection, simultaneously.

$$\min T_{total} \quad (7)$$

$$\text{s.t. } T_{total} \geq T_c^{VSB} - \sum_{i=1}^n R_{ic} \cdot a_i \quad \forall c \in P \quad (7a)$$

$$x_i + w_{ij} \leq x_j + W(2 + p_{ij} + q_{ij} - a_i - a_j) \quad \forall i, j \quad (7b)$$

$$x_i - w_{ji} \geq x_j - W(3 + p_{ij} - q_{ij} - a_i - a_j) \quad \forall i, j \quad (7c)$$

$$y_i + h_{ij} \leq y_j + H(3 - p_{ij} + q_{ij} - a_i - a_j) \quad \forall i, j \quad (7d)$$

$$y_i - h_{ji} \geq y_j - H(4 - p_{ij} - q_{ij} - a_i - a_j) \quad \forall i, j \quad (7e)$$

$$0 \leq x_i + w_i \leq W, \quad 0 \leq y_i + h_i \leq H \quad \forall i \quad (7f)$$

$$p_{ij}, q_{ij}, a_i : 0-1 \text{ variable} \quad \forall i, j \quad (7g)$$

where a_i indicates whether candidate c_i is on the stencil, p_{ij} and q_{ij} represent the location relationships between c_i and c_j . The number of variables is $O(n^2)$, where n is number of characters. We can see that if $a_i = 0$, constraints (7b) - (7e) are not active. Besides, it is easy to see that when $a_i = a_j = 1$, for each of the four possible choices of $(p_{ij}, q_{ij}) = (0, 0), (0, 1), (1, 0), (1, 1)$, only one of the four inequalities (7b) - (7e) are active. For example, with $(a_i, a_j, p_{ij}, q_{ij}) = (1, 1, 1, 1)$, only the constraint (7e) applies, which allows character c_i to be anywhere above character c_j . The other three constraints (7b)-(7d) are always satisfied for any permitted values of (x_i, y_i) and (x_j, y_j) .

Program (7) can be relaxed to linear programming (LP) by replacing constraint (7g) as:

$$0 \leq p_{ij}, q_{ij}, a_i \leq 1$$

However, similar to the discussion in 1DOSP, the relaxed LP solution provides no information or guideline to the packing, i.e., every a_i is set as 1, and every p_{ij} is set as 0.5. In other words, this LP relaxation provides no useful information to guide future rounding: all the character candidates are selected and no ordering relationship is determined. Therefore we can see that LP rounding method cannot be effectively applied to program (7).

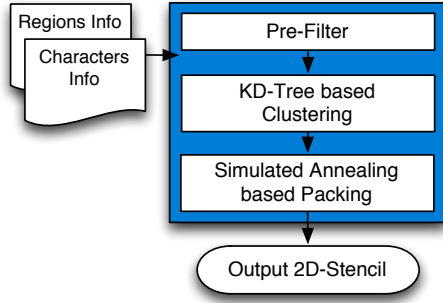


Fig. 9. E-BLOW overall flow for 2DOSP.

4.2 Clustering based Simulated Annealing

To deal with all these limitations of ILP formulation, a fast packing framework is proposed (see Fig. 9). Given the input character candidates, the pre-filter process is first applied to remove characters with bad profit (defined in (6)). Then the second step is a clustering algorithm to effectively speed-up the design process. Followed by the final floorplanner to pack all candidates.

Clustering is a well studied problem, and there are many of works and applications in VLSI [36]. However, previous methodologies cannot be directly applied here. First, traditional clustering is based on netlist, which provides the all clustering options. Generally speaking, netlist is sparse, but in OSP the connection relationships are so complex that any two characters can be clustered, and totally there are $O(n^2)$ clustering options. Second, given two candidates c_i and c_j , there are several clustering options. For example, horizontal clustering and vertical clustering may have different overlapping blank space.

The main ideas of our clustering are iteratively search and group each character pair (c_i, c_j) with similar blank spaces, profits, and sizes. Character c_i is said to be similar to c_j , if the following condition is satisfied:

$$\begin{cases} \max\{|w_i - w_j|/w_j, |h_i - h_j|/h_j\} \leq bound \\ \max\{|sh_i - sh_j|/sh_j, |sv_i - sv_j|/sv_j\} \leq bound \\ |profit_i - profit_j|/profit_j \leq bound \end{cases} \quad (8)$$

where w_i and h_i are the width and height of c_i . sh_i and sv_i are the horizontal blank space and vertical blank space of c_i , respectively. In our implementation, $bound$ is set as 0.2. We can see that in clustering, all the size, blanks, and profits are considered.

The details of our clustering procedure are shown in Algorithm 4. First all the initial character candidates are sorted by $profit_i$ (line 2), so those characters with more shot number reduction are tend to be clustered. Then all characters are labeled as *unclustered* (line 3). The clustering (lines 3-10) is repeated until no characters can be further merged. When cluster c_i, c_j , the information of c_i is modified to incorporate c_j , and the c_j is labeled as *clustered*.

Algorithm 4 KD-Tree based Clustering

Require: set of character candidates.

- 1: Sort all candidates by $profit_i$;
 - 2: Set each candidates c_i to *unclustered*;
 - 3: **repeat**
 - 4: **for all** unclustered candidate c_i **do**
 - 5: **if** can find similar unclustered character c_j
 - 6: **then**
 - 7: Update information of c_i to incorporate c_j ;
 - 8: Label c_j as *clustered*;
 - 9: **end if**
 - 10: **end for**
 - 11: **until** no character can be merged
-

For each candidate c_i , finding available c_j may need $O(n)$, and complexity of the horizontal clustering and vertical clustering are both $O(n^2)$. Then the complexity of the whole procedure is $O(n^2)$, where n is the number of candidates.

A KD-Tree [37] is used to speed-up the process of finding available pair (c_i, c_j) . It provides fast $O(\log n)$ region searching operations which keeping the time for insertion and deletion small: insertion, $O(\log n)$; deletion of the root, $O(n(k-1)/k)$; deletion of a random node, $O(\log n)$. Using KD-Tree, the complexity of the Algorithm 4 can be reduced to $O(n \log n)$. For instance, given nine character candidates $\{c_1, \dots, c_9\}$ as in Fig. 10 (a), the corresponding KD-Tree is shown in Fig. 10 (b). Note that KD-Tree can store multiple dimensional vertices, thus a single tree is enough to store all the information regarding width, height, blank spaces, and profits. For the sake of convenience, here characters are distributed only based on horizontal and vertical blank spaces. Thus only two dimensional space is illustrated in Fig. 10 (a). To search candidates with similar blank space with c_2 (see the shaded region of Fig. 10 (a)), it may need $O(n)$ time to scan all candidates, where n is the total candidate number. However, under the KD-Tree structure, this search procedure can be resolved in $O(\log n)$. All candidates scanned ($c_1 - c_5$) are illustrated in Fig. 10 (b). Particularly, after scanning the c_5 , since c_5 is out of the search range, we can make sure the whole sub-tree rooted by c_7 is out of the search range as well.

In [24], the 2DOSP is transformed into a fixed-outline floorplanning problem. If a character candidate is outside the fixed-outline, then the character would not be prepared on stencil. Otherwise, the character candidate would be selected and packed on stencil. Parquet [38] was adopted as simulated annealing engine, and Sequence Pair [39] was used as a topology representation. In E-BLOW we apply a simulated annealing based framework similar to that in [24]. To demonstrate the effectiveness of our pre-filter and clustering methodologies, E-BLOW uses the same parameters.

TABLE 3
Result Comparison for 1DOSP

	char #	CP #	Greedy in [24]			[24]			[25]			E-BLOW		
			T	char#	CPU(s)	T	char#	CPU(s)	T	char#	CPU(s)	T	char#	CPU(s)
1D-1	1000	1	64891	912	0.1	50809	926	13.5	19095	940	0.005	19479	940	2.1
1D-2	1000	1	99381	884	0.1	93465	854	11.8	35295	864	0.005	34974	866	1.7
1D-3	1000	1	165480	748	0.1	152376	749	9.13	69301	757	0.005	67209	766	1.7
1D-4	1000	1	193881	691	0.1	193494	687	7.7	92523	703	0.005	93816	703	4.5
1M-1	1000	10	63811	912	0.1	53333	926	13.5	39026	938	0.01	37848	944	3.8
1M-2	1000	10	104877	884	0.1	95963	854	11.8	77997	864	0.01	75303	874	3.5
1M-3	1000	10	172834	748	0.1	156700	749	9.2	138256	758	0.56	132773	774	9.3
1M-4	1000	10	200498	691	0.1	196686	687	7.7	176228	698	0.36	173193	711	7.4
1M-5	4000	10	274992	3604	1.0	255208	3629	1477.3	204114	3660	0.03	202401	3680	37.9
1M-6	4000	10	437088	3341	1.0	417456	3346	1182	357829	3382	0.03	348007	3420	48.4
1M-7	4000	10	650419	3000	1.0	644288	2986	876	568339	3016	0.59	563054	3064	54.0
1M-8	4000	10	820013	2756	1.0	809721	2734	730.7	731483	2760	0.42	721149	2818	54.7
Avg. Ratio	-	-	270680.4	1597.6	0.4	259958.3	1594.0	362.5	209123.8	1611.7	0.17	205767.2	1630.7	16.6
			1.32	0.98	0.02	1.26	0.98	19.01	1.02	0.99	0.01	1.0	1.0	1.0

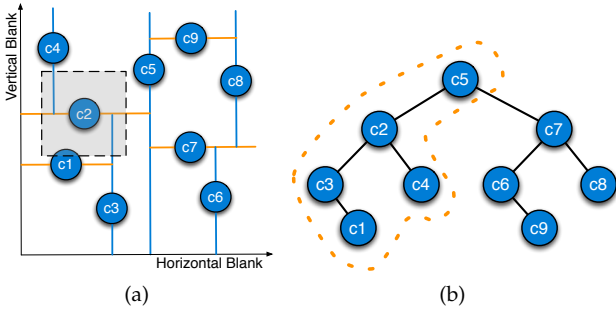


Fig. 10. KD-Tree based region searching. (a) A two dimensional space split by eight points; (b) The corresponding two dimensional KD-Tree.

5 EXPERIMENTAL RESULTS

E-BLOW is implemented in C++ programming language and executed on a Linux machine with two 3.0GHz CPU and 32GB Memory. GUROBI [40] is used to solve ILP/LP. The benchmark suite from [24] are tested (1D-1, ..., 1D-4, 2D-1, ..., 2D-4). To evaluate the algorithms for MCC system, eight benchmarks (1M-x) are generated for 1DOSP and the other eight (2M-x) are generated for the 2DOSP problem. In these new benchmarks, character projection (CP) number are all set to 10. For each small case (1M-1, ..., 1M-4, 2M-1, ..., 2M-4) the character candidate number is 1000, and the stencil size is set to $1000\mu m \times 1000\mu m$. For each larger case (1M-5, ..., 1M-8, 2M-5, ..., 2M-8) the character candidate number is 4000, and the stencil size is set to $2000\mu m \times 2000\mu m$. The size and the blank width of each character are similar to those in [24]. It shall be noted that [24] is aimed for single CP system, for MCC system it is modified to optimize the total writing time of all the regions.

5.1 Comparison for 1DOSP

For 1DOSP, Table 3 compares E-BLOW with the greedy method in [24], the heuristic framework in [24], and the algorithms in [25]. We have obtained the programs of [24]

and executed them in our machine. The results of [25] are directly from their paper. Column "char #" is number of character candidates, and column "CP#" is number of character projections. For each algorithm, we report "T", "char#" and "CPU(s)", where "T" is the writing time of the E-Beam system, "char#" is the character number on final stencil, and "CPU(s)" reports the runtime. From Table 3 we can see E-BLOW achieves better performance than both greedy method and heuristic method in [24]. Compared with E-BLOW, the greedy method has 32% more system writing time, while [24] introduces 27% more system writing time. One possible reason is that different from the greedy/heuristic methods, E-BLOW proposes mathematical formulations to provide global view. Additionally, due to the successive rounding scheme, E-BLOW is around $22\times$ faster than the work in [24].

E-BLOW is further compared with one recent 1DOSP solver [25] in Table 3. E-BLOW found stencil placements with best E-Beam system writing time for 10 out of 12 test cases. In addition, for all the MCC system cases (1M-1, ..., 1M-8) E-BLOW outperforms [25]. One possible reason is that to optimize the overall throughput of the MCC system, a global view is necessary to balance the throughputs among different regions. E-BLOW utilizes the mathematical formulations to provide such global optimization. Although the linear programming solvers are more expensive than the deterministic heuristics in [25], the runtime of E-BLOW is reasonable that each case can be finished in 20 seconds on average.

We further demonstrate the effectiveness of the fast ILP convergence (Section 3.3) and post-insertion (Section 3.5). We denote **E-BLOW-0** as E-BLOW without these two techniques, and denote **E-BLOW-1** as E-BLOW with these techniques. Fig. 11 and Fig. 12 compare E-BLOW-0 and E-BLOW-1, in terms of system writing time and runtime, respectively. From Fig. 11 we can see that applying fast ILP convergence and post-insertion can effectively E-Beam system throughput, that is, averagely 9% system writing time reduction can be achieved. In addition, Fig.

12 demonstrates the performance of the fast ILP convergence (see Section 3.3). We can see that in 11 out of 12 test cases, the fast ILP convergence can effectively reduce E-BLOW CPU time. The possible reason for the slow down in case 1D-4 is that when fast convergence is called, if there are still many unsolved a_{ij} variables, ILP solver may suffer from runtime overhead problem. However, if more successive rounding iterations are applied before ILP convergence, less runtime can be reported.

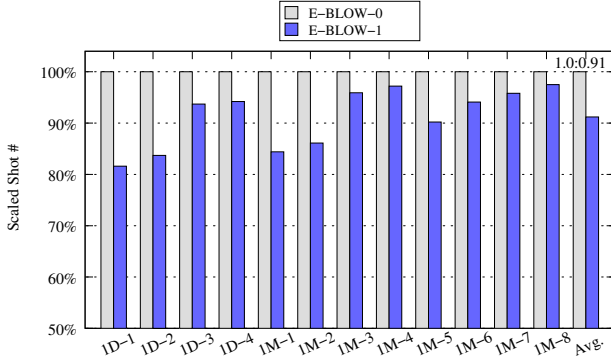


Fig. 11. The comparison of E-Beam system writing times between E-BLOW-0 and E-BLOW-1.

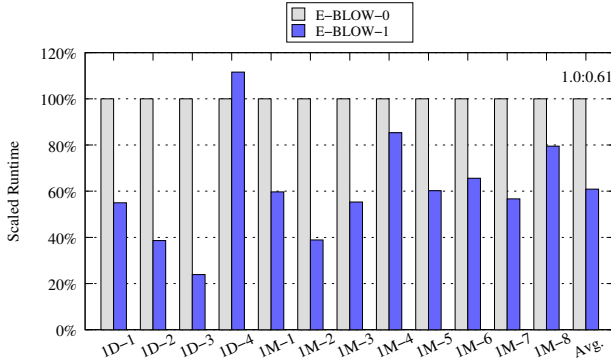


Fig. 12. The comparison of runtime between E-BLOW-0 and E-BLOW-1.

5.2 Comparison for 2DOSP

For 2DOSP, Table 4 gives the similar comparison. For each algorithm, we also record “T”, “char #” and “CPU(s)”, where the meanings are the same with that in Table 3. Compared with E-BLOW, although the greedy algorithm is faster, its design results would introduce 41% more system writing time. Furthermore, compared with E-BLOW, although the framework in [24] puts 2% characters onto stencil, it gets 15% more system writing time. The possible reason is that in E-BLOW the characters with similar writing time are clustered together. The clustering method can help to speed-up the packaging, so E-BLOW is 28× faster than [24]. In addition, after clustering the character number can be reduced. With smaller solution space, the simulated annealing engine

is easier to achieve a better solution, in terms of system writing time.

From both tables we can see that compared with [24], E-BLOW can achieve a better tradeoff between runtime and system throughput.

5.3 E-BLOW vs. ILP

We further compare the E-BLOW with the ILP formulations (3) and (7). Although for both OSP problems the ILP formulations can find optimal solutions theoretically, they may suffer from runtime overhead. Therefore, we randomly generate nine small benchmarks, five for 1DOSP (“1T-x”) and four for 2DOSP (“2T-x”). The sizes of all the character candidates are set to $40\mu m \times 40\mu m$. For 1DOSP benchmarks, the row number is set to 1, and the row length is set to 200. The comparisons are listed in Table 5, where column “candidate#” is the number of character candidates. “ILP” and “E-BLOW” represent the ILP formulation and our E-BLOW framework, respectively. In ILP formulation, column “binary#” gives the binary variable number. For each mode, we report “T”, “char#” and “CPU(s)”, where “T” is E-Beam system writing time, “char#” is character number on final stencil, and “CPU(s)” is the runtime. Note that in Table 5 the ILP solutions are optimal.

Let us compare E-BLOW with ILP formulation for 1D cases (1T-1, ..., 1T-5). E-BLOW can achieve the same results with ILP formulations, meanwhile it is very fast that all cases can be finished in 0.2 seconds. Although ILP formulation can achieve optimal results, it is very slow that a case with 14 character candidates (1T-5) can not be solved in one hour. Next, let us compare E-BLOW with ILP formulation for 2D cases (2T-1, ..., 2T-4). For 2D cases ILP formulations are slow that if the character candidate number is 12, it cannot finish in one hour. E-BLOW is fast, but with some solution quality penalty.

Although the integral variable number for each case is not huge, we find that in the ILP formulations, the solutions of corresponding LP relations are vague. Therefore, expensive search method may cause unacceptable runtimes. From these cases ILP formulations are impossible to be directly applied in OSP problem, as in MCC system character number may be as large as 4000.

6 CONCLUSION

In this paper, we have proposed E-BLOW, a tool to solve OSP problem in MCC system. For 1DOSP, a successive relaxation algorithm and a dynamic programming based refinement are proposed. For 2DOSP, a KD-Tree based clustering method is integrated into simulated annealing framework. Experimental results show that compared with previous works, E-BLOW can achieve better performance in terms of shot number and runtime, for both MCC system and traditional EBL system. Note that the extra cost for multiple stencils is mostly the cost of multiple stencil design, thus different regions tend to have

TABLE 4
Result Comparison for 2DOSP

	char #	CP #	Greedy in [24]			[24]			E-BLOW		
			T	char #	CPU(s)	T	char #	CPU(s)	T	char #	CPU(s)
2D-1	1000	1	159654	734	2.1	107876	826	329.6	105723	789	65.5
2D-2	1000	1	269940	576	2.4	166524	741	278.1	170934	657	52.5
2D-3	1000	1	290068	551	2.6	210496	686	296.7	178777	663	56.4
2D-4	1000	1	327890	499	2.7	240971	632	301.7	179981	605	54.7
2M-1	1000	1	168279	734	2.1	122017	811	313.7	91193	777	58.6
2M-2	1000	1	283702	576	2.4	187235	728	286.1	163327	661	48.7
2M-3	1000	1	298813	551	2.6	235788	653	289.0	162648	659	52.3
2M-4	1000	1	338610	499	2.7	270384	605	285.6	195469	590	53.3
2M-5	4000	10	824060	2704	19.0	700414	2913	3891.0	687287	2853	59.0
2M-6	4000	10	1044161	2388	20.2	898530	2624	4245.0	717236	2721	60.7
2M-7	4000	10	1264748	2101	21.9	1064789	2410	3925.5	921867	2409	57.1
2M-8	4000	10	1331457	2011	22.8	1176700	2259	4550.0	1104724	2119	57.7
Avg.	-	-	550115	1218.1	8.3	448477	1324	1582.7	389930.5	1291.9	56.375
Ratio	-	-	1.41	0.94	0.15	1.15	1.02	28.1	1.0	1.0	1.0

TABLE 5
ILP v.s. EBLOW

	candidate#	ILP				E-BLOW		
		binary#	T	char#	CPU(s)	T	char#	CPU(s)
1T-1	8	64	434	6	0.5	434	6	0.1
1T-2	10	100	1034	6	26.1	1034	6	0.2
1T-3	11	121	1222	6	58.3	1222	6	0.2
1T-4	12	144	1862	6	1510.4	1862	6	0.2
1T-5	14	196	NA	NA	>3600	2758	6	0.1
2T-1	6	66	60	6	37.3	207	5	0.1
2T-2	8	120	354	6	40.2	653	7	0.1
2T-3	10	190	1050	6	436.8	4057	4	0.1
2T-4	12	276	NA	NA	>3600	4208	5	0.2

specific stencils to improve the throughput. However, if a shared stencil is well-designed and optimized that such sharing can achieve very comparable throughput, we can even reduce the stencil design cost. In that situation, sharing stencil design could be attractive, especially for the companies that have limited design budget. As EBL, including MCC system, are widely used for mask making and also gaining momentum for direct wafer writing, we believe a lot more research can be done for not only stencil planning, but also EBL aware design.

ACKNOWLEDGMENT

This work is supported in part by NSF grants CCF-0644316 and CCF-1218906, SRC task 2414.001, NSFC grant 61128010, and IBM Scholarship. The authors would like to thank Prof. Shiyang Hu at Michigan Technological University and Zhao Song at University of Texas for helpful comments.

REFERENCES

- [1] A. B. Kahng, C.-H. Park, X. Xu, and H. Yao, "Layout decomposition for double patterning lithography," in *IEEE/ACM International Conference on Computer-Aided Design (ICCAD)*, 2008, pp. 465–472.
- [2] H. Zhang, Y. Du, M. D. Wong, and R. Topaloglu, "Self-aligned double patterning decomposition for overlay minimization and hot spot detection," in *IEEE/ACM Design Automation Conference (DAC)*, 2011, pp. 71–76.
- [3] B. Yu, K. Yuan, B. Zhang, D. Ding, and D. Z. Pan, "Layout decomposition for triple patterning lithography," in *IEEE/ACM International Conference on Computer-Aided Design (ICCAD)*, 2011, pp. 1–8.
- [4] B. Yu and D. Z. Pan, "Layout decomposition for quadruple patterning lithography and beyond," in *IEEE/ACM Design Automation Conference (DAC)*, 2014, pp. 1–6.
- [5] D. Z. Pan, B. Yu, and J.-R. Gao, "Design for manufacturing with emerging nanolithography," *IEEE Transactions on Computer-Aided Design of Integrated Circuits and Systems (TCAD)*, vol. 32, no. 10, pp. 1453–1472, 2013.
- [6] Y. Arisawa, H. Aoyama, T. Uno, and T. Tanaka, "EUV flare correction for the half-pitch 22nm node," in *Proceedings of SPIE*, vol. 7636, 2010.
- [7] L.-W. Chang, X. Bao, B. Chris, and H.-S. Philip Wong, "Experimental demonstration of aperiodic patterns of directed self-assembly by block copolymer lithography for random logic circuit layout," in *IEEE International Electron Devices Meeting (IEDM)*, 2010.
- [8] H. C. Pfeiffer, "New prospects for electron beams as tools for semiconductor lithography," in *Proceedings of SPIE*, vol. 7378, 2009.
- [9] A. Fujimura, "Design for E-Beam: design insights for direct-write maskless lithography," in *Proceedings of SPIE*, vol. 7823, 2010.
- [10] T. Maruyama, M. Takakuwa, Y. Kojima, Y. Takahashi, K. Yamada, J. Kon, M. Miyajima, A. Shimizu, Y. Machida, H. Hoshino, H. Takita, S. Sugatani, and H. Tsuchikawa, "EBDW technology for EB shuttle at 65nm node and beyond," in *Proceedings of SPIE*, vol. 6921, 2008.
- [11] H. Yasuda, T. Haraguchi, and A. Yamada, "A proposal for an MCC (multi-column cell with lotus root lens) system to be used

- as a mask-making e-beam tool," in *Proceedings of SPIE*, vol. 5567, 2004.
- [12] T. Maruyama, Y. Machida, S. Sugatani, H. Takita, H. Hoshino, T. Hino, M. Ito, A. Yamada, T. Iizuka, S. Komatsue, M. Ikeda, and K. Asada, "CP element based design for 14nm node EBDW high volume manufacturing," in *Proceedings of SPIE*, vol. 8323, 2012.
- [13] M. Shoji, T. Inoue, and M. Yamabe, "Extraction and utilization of the repeating patterns for CP writing in mask making," in *Proceedings of SPIE*, vol. 7748, 2010.
- [14] J.-R. Gao, B. Yu, and D. Z. Pan, "Self-aligned double patterning layout decomposition with complementary e-beam lithography," in *IEEE/ACM Asia and South Pacific Design Automation Conference (ASPDAC)*, Jan 2014, pp. 143–148.
- [15] Y. Du, H. Zhang, M. D. Wong, and K.-Y. Chao, "Hybrid lithography optimization with e-beam and immersion processes for 16nm 1D gridded design," in *IEEE/ACM Asia and South Pacific Design Automation Conference (ASPDAC)*, 2012, pp. 707–712.
- [16] S. Babin, A. B. Kahng, I. I. Mandoiu, and S. Muddu, "Resist heating dependence on subfield scheduling in 50kV electron beam maskmaking," in *Proceedings of SPIE*, vol. 5130, 2003.
- [17] S.-Y. Fang, W.-Y. Chen, and Y.-W. Chang, "Graph-based subfield scheduling for electron-beam photomask fabrication," *IEEE Transactions on Computer-Aided Design of Integrated Circuits and Systems (TCAD)*, vol. 32, no. 2, pp. 189–201, 2013.
- [18] A. B. Kahng, X. Xu, and A. Zelikovsky, "Fast yield-driven fracture for variable shaped-beam mask writing," in *Proceedings of SPIE*, vol. 6283, 2006.
- [19] X. Ma, S. Jiang, and A. Zakhor, "A cost-driven fracture heuristics to minimize sliver length," in *Proceedings of SPIE*, vol. 7973, 2011.
- [20] B. Yu, J.-R. Gao, and D. Z. Pan, "L-Shape based layout fracturing for E-Beam lithography," in *IEEE/ACM Asia and South Pacific Design Automation Conference (ASPDAC)*, 2013, pp. 249–254.
- [21] P. Du, W. Zhao, S.-H. Weng, C.-K. Cheng, and R. Graham, "Character design and stamp algorithms for character projection electron-beam lithography," in *IEEE/ACM Asia and South Pacific Design Automation Conference (ASPDAC)*, 2012, pp. 725–730.
- [22] R. Ikeno, T. Maruyama, T. Iizuka, S. Komatsu, M. Ikeda, and K. Asada, "High-throughput electron beam direct writing of VIA layers by character projection using character sets based on one-dimensional VIA arrays with area-efficient stencil design." in *IEEE/ACM Asia and South Pacific Design Automation Conference (ASPDAC)*, 2013, pp. 255–260.
- [23] M. Sugihara, T. Takata, K. Nakamura, R. Inanami, H. Hayashi, K. Kishimoto, T. Hasebe, Y. Kawano, Y. Matsunaga, K. Murakami, and K. Okumura, "Cell library development methodology for throughput enhancement of character projection equipment," *IEICE Transactions on Electronics*, vol. E89-C, pp. 377–383, 2006.
- [24] K. Yuan, B. Yu, and D. Z. Pan, "E-Beam lithography stencil planning and optimization with overlapped characters," *IEEE Transactions on Computer-Aided Design of Integrated Circuits and Systems (TCAD)*, vol. 31, no. 2, pp. 167–179, Feb. 2012.
- [25] J. Kuang and E. F. Young, "A highly-efficient row-structure stencil planning approach for E-Beam lithography with overlapped characters," in *ACM International Symposium on Physical Design (ISPD)*, 2014.
- [26] C. Chu and W.-K. Mak, "Flexible packed stencil design with multiple shaping apertures for e-beam lithography," in *IEEE/ACM Asia and South Pacific Design Automation Conference (ASPDAC)*, 2014, pp. 137–142.
- [27] W.-K. Mak and C. Chu, "E-Beam lithography character and stencil co-optimization," *IEEE Transactions on Computer-Aided Design of Integrated Circuits and Systems (TCAD)*, vol. 33, 2014.
- [28] D. Guo, Y. Du, and M. D. Wong, "Polynomial time optimal algorithm for stencil row planning in E-Beam lithography," in *IEEE/ACM Asia and South Pacific Design Automation Conference (ASPDAC)*, 2015.
- [29] S. Manakli, H. Komami, M. Takizawa, T. Mitsuhashi, and L. Pain, "Cell projection use in mask-less lithography for 45nm & 32nm logic nodes," in *Proceedings of SPIE*, vol. 7271, 2009.
- [30] S. Arora and B. Barak, *Computational Complexity: A Modern Approach*. Cambridge University Press, 2009.
- [31] S. Martello and P. Toth, *Knapsack Problems: Algorithms and Computer Implementations*. John Wiley & Sons, Inc., 1990.
- [32] M. Dawande, J. Kalagnanam, P. Keskinocak, F. Salman, and R. Ravi, "Approximation algorithms for the multiple knapsack problem with assignment restrictions," *Journal of Combinatorial Optimization*, vol. 4, pp. 171–186, 2000.
- [33] E. L. Johnson, G. L. Nemhauser, and M. W. Savelsbergh, "Progress in linear programming-based algorithms for integer programming: An exposition," *INFORMS Journal on Computing*, vol. 12, no. 1, pp. 2–23, 2000.
- [34] Z. Galil, "Efficient algorithms for finding maximum matching in graphs," *ACM Computing Surveys*, vol. 18, no. 1, pp. 23–38, Mar. 1986.
- [35] S. Sutanthavibul, E. Shragowitz, and J. Rosen, "An analytical approach to floorplan design and optimization," *IEEE Transactions on Computer-Aided Design of Integrated Circuits and Systems (TCAD)*, vol. 10, no. 6, pp. 761–769, Jun 1991.
- [36] C. J. Alpert and A. B. Kahng, "Recent directions in netlist partitioning: a survey," *Integration, the VLSI Journal*, vol. 19, pp. 1–81, August 1995.
- [37] J. L. Bentley, "Multidimensional binary search trees used for associative searching," *Communications of the ACM*, vol. 18, pp. 509–517, September 1975.
- [38] S. N. Adya and I. L. Markov, "Fixed-outline floorplanning: Enabling hierarchical design," *IEEE Transactions on Very Large Scale Integration Systems (TVLSI)*, vol. 11, no. 6, pp. 1120–1135, 2003.
- [39] H. Murata, K. Fujiyoshi, S. Nakatake, and Y. Kajitani, "VLSI module placement based on rectangle-packing by the sequence-pair," *IEEE Transactions on Computer-Aided Design of Integrated Circuits and Systems (TCAD)*, vol. 12, pp. 1518–1524, 1996.
- [40] Gurobi Optimization Inc., "Gurobi optimizer reference manual," <http://www.gurobi.com>, 2014.

APPENDIX

PROOF OF THEOREM 1

Lemma 5. *BSS problem is in NP.*

Proof: It is easy to see that BSS problem is in NP. Given a subset of integer numbers $S' \in S$, we can add them up and verify that their sum is s in polynomial time. \square

Lemma 6. $3SAT \leq_p BSS$.

Proof: In 3SAT problem, we are given m clauses $\{C_1, C_2, \dots, C_m\}$ over n variables $\{y_1, y_2, \dots, y_n\}$. Besides, there are three literals in each clause, which is the OR of some number of literals. Eqn. (9) gives one example of 3SAT, where $n = 4$ and $m = 2$.

$$(y_1 \vee \bar{y}_3 \vee \bar{y}_4) \wedge (\bar{y}_1 \vee y_2 \vee \bar{y}_4) \quad (9)$$

Without loss of generality, we can have the following assumptions:

- 1) No clause contains both variable y_i and \bar{y}_i . Otherwise, any such clause is always true and we can just eliminate them from the formula.
- 2) Each variable y_i appears in at least one clause. Otherwise, we can just assign any arbitrary value to the variable y_i .

To convert a 3SAT instance to a BSS instance, we create two integer numbers in set S for each variable y_i and three integer numbers in S for each clause C_j . All the numbers in set S and s are in base 10. Besides, $10^{n+2m} < y_i < 2 \cdot 10^{n+2m}$, so that the bounded constraints are satisfied. All the details regarding S and s are defined as follows.

- In the set S , all integer numbers are with $n+2m+1$ digits, and the first digit are always 1.
- In the set S , we construct two integer numbers t_i and f_i for the variable y_i . For both of the values, the n digits after the first '1' serve to indicate the corresponding variable in S . That is, the i^{th} digit in these n digits is set to 1 and all others are 0. For the next m digits, the j^{th} digit is set to 1 if the clause C_j contains the respective literal. The last m digits are always 0.
- In the set S , we also construct three integer numbers c_{j1}, c_{j2} and c_{j3} for each clause C_j . In c_{jk} where $k = \{1, 2, 3\}$, the first n digits after the first '1' are 0, and in the next m digits all are 0 except the j^{th} index setting to k . The last m digits are all 0 except the j^{th} index setting to 1.
- $T = (n+m) \cdot 10^{n+2m} + s_0$, where s_0 is an integer number with $n+2m$ digits. The first n digits of s_0 are 1, in the next m digits all are 4, and in the last m digits all are 1.

Based on the above rules, given the 3SAT instance in Eqn. (9) the constructed set S and target s are shown in Fig. 13. Note that the highest digit achievable is 9, meaning that no digit will carry over and interfere with other digits.

Claim 1. *The 3SAT instance has a satisfying truth assignment iff the constructed BSS instance has a subset that adds up to s .*

Proof of \Rightarrow part of Claim: If the 3SAT instance has a satisfying assignment, we can pick a subset containing all t_i for which y_i is set to true and f_i for which y_i is set to false. We should then be able to achieve s by picking the necessary c_{jk} to get 4's in the s . Due to the last m '1' in s , for each $j \in [m]$ only one would be selected from $\{c_{j1}, c_{j2}, c_{j3}\}$. Besides, we can see totally $n+m$ numbers would be selected from S .

Proof of \Leftarrow part of Claim: If there is a subset $S' \in S$ that adds up to s , we will show that it corresponds to a satisfying assignment in the 3SAT instance. S' must include exactly one of t_i and f_i , otherwise the i^{th} digit value of s_0 cannot be satisfied. If $t_i \in S'$, in the 3SAT we set y_i to true; otherwise we set it to false. Similarly, S' must include exactly one of c_{j1}, c_{j2} and c_{j3} , otherwise

		y_1	y_2	y_3	y_4	C_1	C_2	A_1	A_2
t_1	=	1	1	0	0	0	1	0	0
f_1	=	1	1	0	0	0	0	1	0
t_2	=	1	0	1	0	0	0	1	0
f_2	=	1	0	1	0	0	0	0	0
t_3	=	1	0	0	1	0	0	0	0
f_3	=	1	0	0	1	0	1	0	0
t_4	=	1	0	0	0	1	0	0	0
f_4	=	1	0	0	0	1	1	1	0
c_{11}	=	1	0	0	0	0	1	0	1
c_{12}	=	1	0	0	0	0	2	0	1
c_{13}	=	1	0	0	0	0	3	0	1
c_{21}	=	1	0	0	0	0	0	1	0
c_{22}	=	1	0	0	0	0	0	2	0
c_{23}	=	1	0	0	0	0	0	3	0
s	=	6	1	1	1	1	4	4	1
s_0	=		1	1	1	1	4	4	1

Fig. 13. The constructed BSS instance for the given 3SAT instance in (9).

the last m digits of s cannot be satisfied. Therefore, all clauses in the 3SAT are satisfied and 3SAT has a satisfying assignment. \square

For instance, given a satisfying assignment of Eqn. (9): $\langle y_1 = 0, y_2 = 1, y_3 = 0, y_4 = 0 \rangle$, the corresponding subset S' is $\{f_1 = 110000100, t_2 = 101000100, f_3 = 100101000, f_4 = 100011100, c_{12} = 100002010, c_{21} = 100000101\}$. We set $s = (m+n) \cdot 10^{n+2m} + s_0$, where $s_0 = 11114411$, and then $s = 611114411$. We can see that $f_1 + t_2 + f_3 + f_4 + s_{12} + s_{21} = s$.

Combining Lemma 5 and Lemma 6, we can achieve the following theorem.